

---

Proceedings of the XXXVI International School of Semiconducting Compounds, Jaszowiec 2007

## Modeling of Small Diameter Semiconductor Nanowires

M. BUKAŁA, M. GALICKA, R. BUCZKO AND P. KACMAN

Institute of Physics, Polish Academy of Sciences  
al. Lotników 32/46, 02-668 Warsaw, Poland

The properties of very thin (up to 16 Å diameter) wires, cut out from the bulk in either zinc-blende or wurtzite material, are studied theoretically. In the total energy calculations we use *ab initio* methods and consider three different crystallographic growth axes for the zinc-blende and one for the wurtzite structure. We show that the most stable zinc-blende nanowires are those growing along (111) direction, however, the wurtzite structure is found to be energetically more favorable than the zinc-blende for wires of the same diameter. In addition, the band structure of the wires was calculated.

PACS numbers: 73.21.Hb, 73.43.Cd, 73.61.Ey

### 1. Introduction

The fabrication of quantum wires has been a challenge for several decades [1–4]. A few years ago a great renewed interest in this field emerged, stimulated by the reports of successful growth of single crystal free-standing III–V nanowires, [5–7]. The semiconductor nanowires (NWs) are attracting considerable attention because they represent a unique system for exploring phenomena at the nanoscale and also due to their potential applications. The one-dimensional nanostructures are expected to play a critical role in future electronic and optoelectronic devices — recent experiments have proved already that semiconductor NWs can be used as building-blocks of various electronic devices, including FETs, *p–n* diodes, bipolar junction transistors, as well as chemical and biological sensors.

The growth of small-diameter structures raises the question of the limit of a bulk-like description of bonding in NWs, since for small enough diameters, the predominance of surface atoms over inner (bulk-like) atoms will eventually lead to bonds and structures distinct from those of the bulk system. In this paper we present the results of *ab initio* simulations undertaken to study these effects and to investigate the stability of NWs in different configurations.

## 2. Model nanowires — surface reconstruction

We consider infinite GaAs NWs of both, the zinc-blende (*zb*) and wurtzite (*wz*) structure, at zero pressure and zero temperature. The studied NWs have diameters ranging from 6 to 16 Å and are oriented along different crystallographic axes. Our model NWs are cut-out from the bulk GaAs: in the *zb* structure along the three: (001), (110), and (111) crystallographic directions; in the *wz* structure along the (0001) axis. The unit cell for the *wz* NW grown along (0001) axis corresponds to *zb* (111) NW unit cell, with the height in the growth direction reduced to  $\frac{2}{3}$  — this reduction leads, of course, to the change of the stacking, from the *zb* ABC to the *wz* AB alignment. The periodic boundary conditions are employed along the NW axis. Due to the calculation method described below we use also periodic conditions in the two other directions with the unit cell dimensions assuring that a minimum separation between neighboring wires is not less than 6 Å. This creates, in effect, the net of separated continuous wires. The examples of the wires constructed in the way described above are shown in the (a) and (b) parts of the first four figures — *zb* NWs for different crystallographic directions are presented in Fig. 1, Fig. 2, and Fig. 3, and the *wz* NW in Fig. 4.

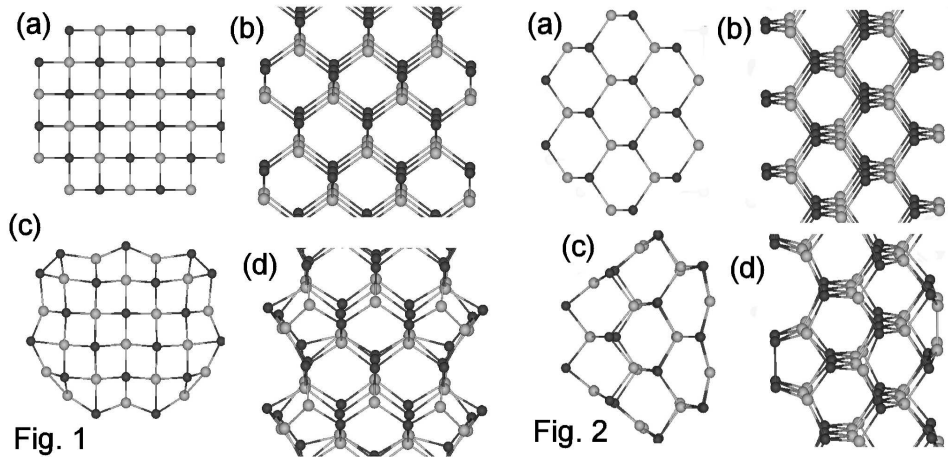


Fig. 1. The GaAs NWs along (001) direction in the *zb* with the diameter about 13 Å. The gray and black circles denote Ga and As atoms, respectively. The NW before the relaxation — the top (a) and side (b) view. The NW after the relaxation — the view from the top (c) and from the side (d).

Fig. 2. The same as for Fig. 1, but along (110) direction.

Then, we use first-principle methods to determine the minimum energy atomic configuration of each of the initial structures. We allow for relaxation of all atomic positions and of the unit cell dimension along the NW axis. The resulting structures are shown in the parts (c) and (d) of the same figures. The main

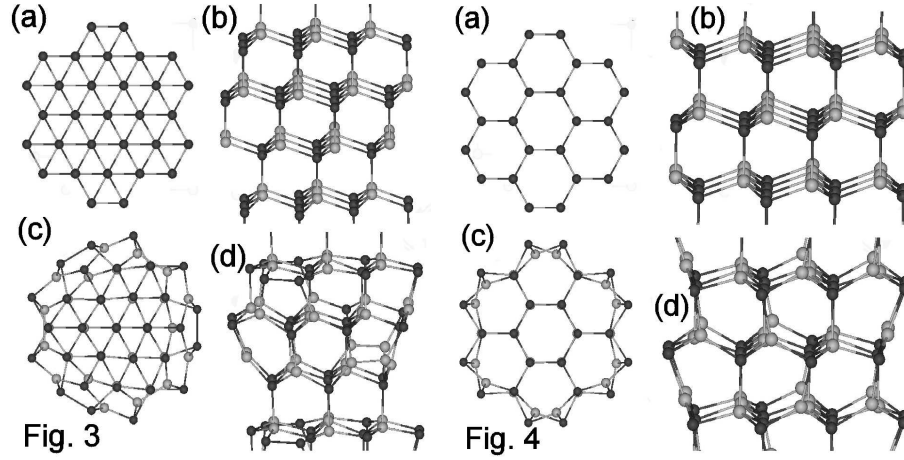


Fig. 3. The same as for Fig. 1, but along (111) direction.

Fig. 4. The same as for Fig. 1, but along (0001) direction in the  $wz$ .

visible effect of the relaxation procedure is the interatomic bonding reconstruction at the NW surface. As one can see in the figures, the shape of the NW surface changes considerably after the relaxation. This is mainly due to the change of positions of Ga atoms, which during the surface reconstruction are tending to the planar configuration (compare the figures).

The reported here *ab initio* total energy calculations are carried out using the ABINIT code [8, 9]. The method is based on the density functional theory (DFT), which adopts a plane wave basis set (we have used the set with a 12 Ha (24 Ry) cut-off energy). For the atomic cores we have used norm-conserving nonlocal Fritz-Haber Institute pseudopotentials generated thanks to FHI98pp code [10]. The  $k$ -points are generated only within the irreducible Brillouin zone. The density of  $k$ -points in the Brillouin zone is 50 [ $\text{\AA}^3$ ]. The exchange correlation energy is calculated using the generalized gradient approximation and the atomic coordinates are relaxed with a conjugate gradient technique using the Broyden-Fletcher-Goldfarb-Shanno (BFGS) minimization [11]. The determined equilibrium configurations are based on the criterion that the maximum force is smaller than 0.03 eV/ $\text{\AA}$ .

In order to find the most energetically favorable nanowire structures we compare their, so-called, wire free energies per number of Ga-As pairs (for this purpose we limit our study to structures with even number of atoms). This free energy is defined as the difference between total energy of the nanowire and bulk GaAs, divided by the number of Ga-As pairs

$$E_{\text{free}} = E_{\text{Ga-As}}^{\text{wire}} - E_{\text{Ga-As}}^{\text{bulk}}.$$

We note that  $E_{\text{free}}$  is always positive, because it reflects the energy cost of the dangling bonds and the bonding reconstruction at the nanowire surface.

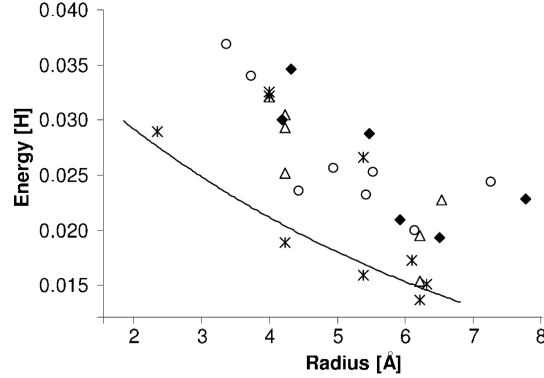


Fig. 5. Dependence of the wire free energy on the NW radius for all studied structures. For *zb* NWs: along (001) — full rhombuses, (110) — open circles, (111) — open triangles. The results for *wz* (0001) NWs are denoted by asterisks.

The impact of the surface reconstruction on the atoms in the wire core adds also to the wire free energy. The thicker the wire, the smaller should be  $E_{\text{free}}$ , as the ratio of the number of atoms at the surface to the total number of atoms in the wire diminishes with the nanowire radius. In Fig. 5 the results of the calculated wire free energy for NW with different radii and structures are collected. In agreement with the expectations,  $E_{\text{free}}$  decreases with the radius of the NW for all structures. However, one should observe that for a given NW radius the lowest free energies have the *wz* NWs. Among the *zb* NWs a comparably low free energy was obtained for the ones with the axis along the (111) direction. These results are in agreement with the fact that most of the experiments report the growth of the III–V semiconductor NWs in the wurtzite (0001) and *zb* (111) structure.

### 3. Band structure

Finally, we choose the relaxed *wz* structures to study the NWs band structure. The calculated energy spectrum for the *wz* NW is presented in Fig. 6 and compared with the band structure in the equivalent direction calculated for the *wz* bulk GaAs, shown in Fig. 7. First, we observe that the obtained energy band gap in the NW is larger about 1 eV than in the bulk. The increase in the band gap in NW is not surprising and seems to result from the confinement. Although it is well known that the DFT accounts incorrectly for the excited electronic states of solids, and hence leads in general too far to small energy band gaps, we believe that this drawback does not affect seriously the difference between the gaps in NW and bulk material. On the other hand, in our calculations we obtain that the band gap increases with increasing diameter of the NWs. This unexpected trend was, however, obtained also previously for SiC NWs and explained in terms of the surface states due to the dangling bonds on the surface of the wires (the

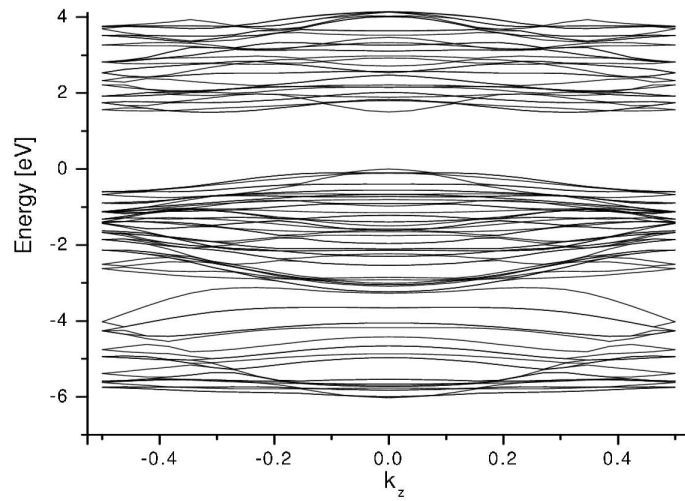


Fig. 6. Band structure of GaAs nanowire wurtzite with the diameter 14 Å.

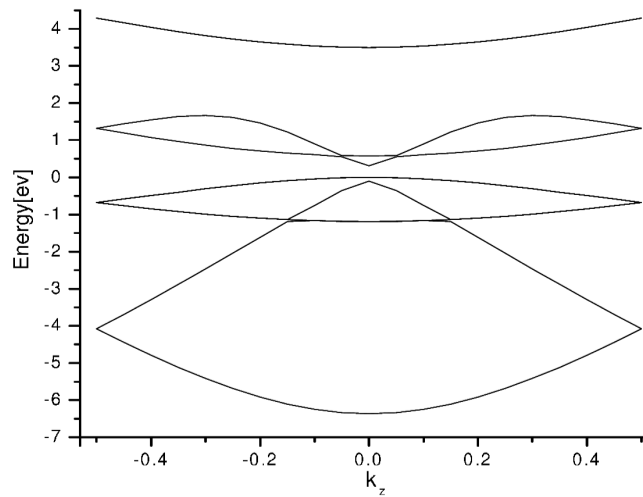


Fig. 7. Band structure of GaAs bulk in the wurtzite structure.

surface states play a predominant role in the smallest diameter wire and result into a dramatic reduction in their band gap) [12].

#### 4. Conclusions

In summary, we have studied theoretically the stability of various GaAs NWs. Our calculations indicate that due to the effects related to the surface reconstruction the (111) direction should be the preferred axis for the growth of stable *zb* nanowires. However, the growth along (0001) in the *wz* structure seems to be the most energetically favorable. The model allowed us also to compute the

band structure of the NWs showing an increase in the band gap as compared to the bulk GaAs and the dependence of the band gap on the NW radius. Although the nanowires considered here are very thin and thus the calculations overestimate the role of the surface, we notice that the obtained results are consistent with the experimentally observed trends.

### Acknowledgments

We thank H. Shtrikman for valuable discussion. This work was partly supported by EU-Transnational Access program, EU project RITA-CT-2003-506095.

### References

- [1] E.I. Givargizov, *J. Cryst. Growth* **31**, 20 (1975).
- [2] P.M. Petroff, A.C. Gossard, W. Wiegmann, *Appl. Phys. Lett.* **45**, 620 (1984).
- [3] R. Bhat, E. Kapon, S. Simhony, E. Colas, D.M. Hwang, N.G. Stoffel, M.A. Koza, *J. Cryst. Growth* **107**, 716 (1991).
- [4] K. Hiruma, M. Yazawa, T. Katsuyama, K. Ogawa, K. Haraguchi, M. Koguchi, H. Kakibayashi, *J. Appl. Phys.* **77**, 447 (1995).
- [5] X. Duan, J. Wang, C.M. Lieber, *Nature (London)* **415**, 617 (2002).
- [6] Y. Xia, P. Yang, Y. Sun, Y. Wub, B. Mayers, B. Gates, Y. Yin, F. Kim, H. Yan, *Adv. Mater. (Weinheim)* **15**, 353 (2003).
- [7] C. Thelander, T. Martensson, M.T. Bjrk, B.J. Ohlsson, M.W. Larsson, L.R. Wallenberg, L. Samuelson, *Appl. Phys. Lett.* **83**, 2052 (2003).
- [8] X. Gonze, J.-M. Beuken, R. Caracas, F. Detraux, M. Fuchs, G.-M. Rignanese, L. Sindic, M. Verstraete, G. Zerah, F. Jollet, M. Torrent, A. Roy, M. Mikami, Ph. Ghosez, J.-Y. Raty, D.C. Allan, *Comput. Mater. Sci.* **25**, 478 (2002).
- [9] X. Gonze, G.-M. Rignanese, M. Verstraete, J.-M. Beuken, Y. Pouillon, R. Caracas, F. Jollet, M. Torrent, G. Zerah, M. Mikami, Ph. Ghosez, M. Veithen, J.-Y. Raty, V. Olevano, F. Bruneval, L. Reining, R. Godby, G. Onida, D.R. Hamann, D.C. Allan, *Z. Kristallogr.* **220**, 558 (2005).
- [10] M. Fuchs, M. Scheffler, *Comput. Phys. Commun.* **119**, 67 (1999).
- [11] W.H. Press, B.P. Flannery, S.A. Teukolsky, W.T. Vetterling, *Numerical Recipes. The Art of Scientific Computing* (FORTRAN Version), Cambridge University Press, Cambridge 1989.
- [12] M. Durandurdu, *Phys. Status Solidi B* **243**, 5 (2006).